Sound quality metrics applied to aircraft components under operational conditions using a microphone array

Merino Martinez, Roberto; Alves Vieira, Ana; Snellen, Mirjam; Simons, Dick

DOI
10.2514/6.2019-2513

Publication date
2019

Document Version
Accepted author manuscript

Published in
25th AIAA/CEAS Aeroacoustics Conference

Citation (APA)
Merino Martinez, R., Alves Vieira, A., Snellen, M., & Simons, D. (2019). Sound quality metrics applied to aircraft components under operational conditions using a microphone array. In *25th AIAA/CEAS Aeroacoustics Conference: 20-23 May 2019 Delft, The Netherlands* [AIAA 2019-2513] https://doi.org/10.2514/6.2019-2513

Sound quality metrics applied to aircraft components under operational conditions using a microphone array

Roberto Merino-Martínez*[1], Ana Vieira†[1], Mirjam Snellen‡[1], and Dick G. Simons§[1]

[1]*Delft University of Technology, 2629 HS Delft, the Netherlands*

Aircraft noise is an increasingly important issue that causes annoyance and complaints for the communities living in the vicinity of airports. The conventional sound metrics (such as the A–weighted sound pressure level) typically used for assessing the impact of aircraft noise often fail to conveniently represent the actual annoyance experienced. More sophisticated sound quality metrics (such as loudness, tonality and sharpness) can be used to determine the psychoacoustic annoyance perceived by the human ear. In this paper, an Airbus A320 landing flyover under operational conditions recorded with a microphone array is analyzed. The application of functional beamforming to the acoustic data allows for the separation of the emissions of different noise sources on board of the aircraft. For this case, the nose landing gear (NLG) and the turbofan engines were selected, due to their expected dominance during approach. It was found that, despite being more quiet than the turbofan engines, the NLG system emits a strong tonal sound that makes it overall more annoying than the noise of the engines. Airframe noise prediction models (Fink's and Guo's methods) do not consider this tone and considerably underpredict the noise levels and the annoyance of the NLG. Thus, it is highly recommended to employ these sound quality metrics to study aircraft noise and to evaluate the potential improvement in annoyance of future low–noise aircraft concepts, rather than just a difference in the sound pressure level in decibels.

I. Introduction

Aircraft noise emissions are a continuous cause of annoyance and complaints for the population living in the surroundings of airports [1] and they can even lead to harmful health effects [2]. In addition, these complaints often limit the capacity and the expansion of airports with the consequent loss of revenue [3]. Even though significant reductions in the noise levels per aircraft have been achieved over the last decades [4], the continuous growth of air traffic (approximately at a 5% rate per year [5]) and stricter noise regulation laws [6] make aircraft noise one of the main issues the aerospace industry has to currently deal with. Therefore, it is essential to obtain accurate information about the aircraft noise characteristics in order to reduce the nuisance of the communities.

Experimental measurements of aircraft noise are typically relatively simple, employing recordings of single microphones [7] and conventional sound metrics, such as the A–weighted sound pressure level ($L_{\mathrm{p,A}}$). Conventional sound metrics can also be more elaborated, such as the effective perceived noise level (EPNL), which also accounts for the duration of the signal and the presence of tones [4]. However, previous research [8–10] showed that conventional noise metrics often fail to fully represent the actual annoyance experienced by the human ear. Therefore, more sophisticated sound quality metrics (SQM) from the field of psychoacoustics are starting to be used for investigating the characteristics of flying aircraft noise [8–12] because they capture

*Postdoctoral researcher, Aircraft Noise & Climate Effects section, Faculty of Aerospace Engineering, Kluyverweg 1. AIAA Student Member. E-mail: r.merinomartinez@tudelft.nl

†PhD candidate, Aircraft Noise & Climate Effects section, Faculty of Aerospace Engineering, Kluyverweg 1. E-mail: a.e.alvesvieira@tudelft.nl

‡Associate professor, Aircraft Noise & Climate Effects section, Faculty of Aerospace Engineering, Kluyverweg 1. E-mail: m.snellen@tudelft.nl

§Full professor, Aircraft Noise & Climate Effects section, Faculty of Aerospace Engineering, Kluyverweg 1. E-mail: d.g.simons@tudelft.nl

the behavior of the human ear in a better way. In the past, these SQM have been employed in the automotive industry [13].

In case multiple microphones are employed simultaneously for the recordings, such as with the so–called phased microphone arrays [3, 14], acoustic imaging methods [15] can be applied in order to localize the different sound sources on the flying aircraft and analyze them separately [1, 16–22]. These devices enable the study of the noise emissions of specific aircraft elements, such as the landing gear system [1, 21, 22] or the turbofan engines [23, 24].

The aim of this paper is to apply the SQM to the sound signals of different aircraft elements extracted via acoustic imaging. The combination of both approaches aims at ascertaining which parts of the aircraft cause the highest annoyance for observers on the ground, which may not necessarily correspond to the elements emitting the highest sound pressure levels. The final goal of this research would be to devote the efforts of noise reduction technologies to the elements causing the highest annoyance.

This procedure is applied to acoustic measurements of commercial aircraft flyovers under operational conditions recorded using a microphone array at Amsterdam Airport Schiphol [18, 19, 23]. In this research, the SQM are calculated when the aircraft is located exactly over the observer. Even though several different aircraft types were recorded, this study is limited to one aircraft type for simplicity: the Airbus A320. For comparing SQM results between different aircraft types, the reader is referred to the paper by Vieria et al. [25]. In the current study, two different noise sources are analyzed due to their expected importance during landing [24, 26]: the nose landing gear (NLG) and the turbofan engines. The NLG system of this aircraft type (and other commercial aircraft) is known to emit a strong tonal component [1, 18, 21, 22], which is most likely caused by the presence of open cavities interacting with the incoming flow [27–30].

In addition, airframe noise prediction models (such as and Fink's [31] and Guo's [32, 33] methods) are used and the frequency spectra and SQM obtained with these models are compared with those calculated experimentally.

A brief explanation of the sound quality metrics considered is given in section II. The experimental setup is described in section III. The acoustic imaging method used, as well as the sound propagation model considered, are explained in section IV. The airframe noise prediction models of Fink and Guo are briefly introduced in section V. Finally, the obtained results are discussed in section VI and the main conclusions are stated in section VII.

II. Sound Quality Metrics (SQM)

As mentioned before, relatively simple sound metrics are typically employed for analyzing aircraft noise. Perhaps the simplest and best–known one is the sound pressure level (SPL or L_p) which is basically a measure of the acoustic pressure referred to a reference pressure (normally the hearing threshold of the human ear, i.e., 20 μPa) [34] expressed in the logarithmic decibel scale. Different kinds of frequency–dependent weighting can be applied to the L_p metric to represent the human ear response in a better way [4]. The most widely used one is the so–called A–weighting, which considerably lowers the influence of low frequencies (below 1 kHz). In case the duration of the sound is also taken into account, the sound exposure level (SEL or $L_{\mathrm{p,A,e}}$) is normally used [4]. Lastly, the EPNL metric introduced in section I accounts for the duration of the sound signal and also for the presence of tonal components [4] by using the one–third–octave band spectrum. However, the EPNL metric was introduced in the 1960s to analyze the noise signatures of the aircraft of that time (mostly equipped with turbojet engines), which are very different from those of modern aircraft.

These *conventional* sound metrics usually fail to accurately capture the annoyance experienced by the communities around airports [9, 10]. Therefore, more sophisticated SQM from the field of psychoacoustics are currently being studied and considered for their use in aircraft noise [8–12]. These metrics aim at representing the actual annoyance experienced by the human ear by including more elaborated calculations [10].

The most commonly used SQM in decreasing order of influence to the experienced annoyance [9] are introduced below. Since the explanation of the complete calculation process of each SQM is quite lengthy, only a brief description is provided here. The interested reader is referred to references [9, 10] for more detailed information about the SQM.

II.A. Loudness

Loudness (N) is the subjective perception of the magnitude of a sound and corresponds to the overall sound intensity [9, 10]. The calculation of loudness has been standarized within the ISO norm 532–1 [35] using Zwicker's method.

This metric considers the spectral characteristics of a sound by dividing the frequency spectrum in critical frequency bands, which are related to the neural activity of the human ear. The potential masking of the loudness in each critical frequency band due to the adjacent critical bands is evaluated and accounted for in order to determine the total *unmasked* loudness N by integrating the whole frequency spectrum considered. The unit of this metric is the phon (when in logarithmic scale) or the sone (in linear scale). An increase of 10 phon corresponds to doubling the value in sone, i.e., a sound 10 phon louder is perceived as twice as loud [4].

II.B. Tonality

The tonality metric (K) measures the perceived strength of the unmasked tonal energy within a complex sound [9, 10, 36]. In this paper Aures' method [36] was employed. Only tones (pure tones and narrow–band tones with a bandwidth lower than a critical frequency bandwidth) that protrude more than a certain L_p excess (typically 7 dB) with respect to the surrounding broadband noise are considered as *aurally relevant* and employed in this method. The potential masking of each tone with respect to the rest of the tones detected (due to secondary neural excitation [36]) and the surrounding broadband noise are evaluated and accounted for. Lastly, all the combined contributions of the relevant tonal components are weighted using a factor that considers the ratio of the loudness of the sound signal with and without tones. The unit of this metric is the tonality unit (t.u.). Tonality ranges from 0 to 1, and it has a value of 1 for a sinusoidal wave with a frequency of 1 kHz and a L_p of 60 dB.

II.C. Sharpness

Sharpness (S) describes the high–frequency content of a sound [9, 10] in terms of the proportion of the loudness at high frequencies with respect to the total loudness in the whole frequency range. In this paper von Bismark's [37] method was used, which weights the loudness levels at frequencies higher than 2900 Hz (i.e., the 16^{th} critical frequency band [35]) stronger as the frequency increases. The unit of this metric is the acum.

II.D. Psychoacoustic annoyance

Since the ultimate purpose of this approach is to obtain a single metric that accurately represents the actual annoyance experienced, combined metrics such as the Psychoacoustic Annoyance (PA) model introduced by Fastl and Zwicker [38] are a suitable option. In this paper, a modified version of the PA metric ($\mathrm{PA_{mod}}$) is employed, which incorporates the tonality following More's recommendations [10]. Other SQM are not considered in this paper, namely roughness [39] and fluctuation strength [38], because they require information about the evolution in time of the sound signal and in this paper only the instant where the aircraft is directly overhead of the observer is considered. This was done mostly due to limitations of the setup and the acoustic imaging method, which provides a considerably worse performance in directions different than the one perpendicular to the array plane [40]. The roughness and fluctuation strength metrics are normally included in the $\mathrm{PA_{mod}}$ metric, but their contributions (especially for the case of aircraft noise) are typically negligible [10]. The work by Vieria et al. [25] studies the SQM of aircraft flyovers using a similar setup but considering the recordings of a single microphone during 10 s. Hence, the influence of roughness and fluctuation strength to the noise annoyance are investigated there.

Therefore, in this paper the same nomenclature for the metric ($\mathrm{PA_{mod}}$) is used, but it should be noted that it only includes the contributions of loudness, tonality and sharpness and is expressed as

$$\mathrm{PA_{mod}} = N\left(1 + \sqrt{-0.16 + 11.46\,\omega_S^2 + 1.25\,\omega_T^2}\right). \tag{1}$$

where the term ω_S contains the sharpness S (and loudness N) contribution:

$$\omega_S = \begin{cases} 0.25(S - 1.75)\log_{10}(N + 10), & \text{for } S \geq 1.75 \\ 0, & \text{for } S < 1.75 \end{cases} \tag{2}$$

and the term ω_T contains the tonality K (and loudness N) contribution:

$$\omega_T = \left(1 - e^{-0.29N}\right)\left(1 - e^{-5.49K}\right). \tag{3}$$

III. Experimental setup

A total of 115 landing aircraft flyovers were recorded in Amsterdam Airport Schiphol using a phased microphone array. Landing operations were considered because turbofan engines normally operate at approach idle in these situations, enabling the identification of airframe noise sources [18]. A 32–microphone array featuring a logarithmic spiral distribution with a 1.7 m diameter was placed 1240 m away from the threshold of the Aalsmeerbaan runway (36R), see Fig. 1. The microphones were PUI Audio POM–2735P–R analog condenser microphones [41] with a sensitivity of -35 ± 2 dB (ref. 1 V/Pa) and a frequency range of 20 Hz to 25 kHz. An optical camera (Datavision UI-1220LE [42] with a Kowa LM4NCL lens recording with at a sampling frequency of 30 Hz) was integrated into the center of the array at a fixed angle facing straight up from the ground, which provided video footage synchronized with the microphone data. The weather conditions during the measurements were very similar and presented low wind speeds [23].

Out of all the recorded flyovers, only 7 Airbus A320 measurements were considered for this paper. The experimental results here presented refer to a single Airbus A320 flyover for brevity reasons, but all the others showed comparable values [24]. As mentioned before, the paper by Vieria et al. [25] analyzes the differences in SQM between several different aircraft types (also including takeoff operations) with a similar setup.

This aircraft type was selected because its NLG system is known to be one of the dominant noise sources during landing [1, 18, 21, 22], due to its strong tonal signature (see Figs. 2a and 2b), which is most probably caused by the presence of open cavities [27–30].

The aircraft trajectories were calculated to account for the propagation effects from the source to the receiver, see section IV below. Data from three different sources [18] were used:

1. The Automatic Dependent Surveillance–Broadcast (ADS–B) (when available).
2. The radar from air traffic control (offered by Amsterdam Airport Schiphol).
3. The extrapolation of the images taken by the optical camera.

The three methods provided very similar results (with variations up to 6%), but the data from the optical camera were employed due to its availability and because it is easier to overlay the acoustic source plots to the pictures. The results from the other two methods were used as a validation. The flight altitude and aircraft velocity above the array for the Airbus A320 flyover presented here were 63.4 m and 81.4 m/s, respectively. Henceforth, true air speeds (considering the wind velocities) are considered in this paper.

The microphone array used a sampling frequency of 40 kHz and band filters to obtain frequencies between 45 Hz and 11,200 Hz. For each measurement, 0.1024 s of data was considered for which the aircraft is approximately overhead of the microphone array center (emission angle of $\theta \approx 90°$, corrected for the source motion). For acoustic imaging purposes, the averaged cross–spectral matrix (CSM) is computed using Welch's method [43] employing data blocks of 2048 samples and Hanning windowing with 50 % data overlap, obtaining a frequency resolution of approximately 20 Hz.

The frequency range selected ranges from 1 kHz to 10 kHz, which is considered to be of interest for aircraft noise research [26]. The lower bound was selected for having sufficient spatial resolution to separate the NLG and the turbofan engines, which are located approximately 15 m apart. Aliasing and the amount of sidelobes in the source map determined the highest frequency of study [3].

IV. Acoustic imaging method and sound propagation

Functional beamforming [44, 45] was employed for processing the acoustic data from the microphone array as it provides better dynamic range and array spatial resolution than conventional beamforming [14],

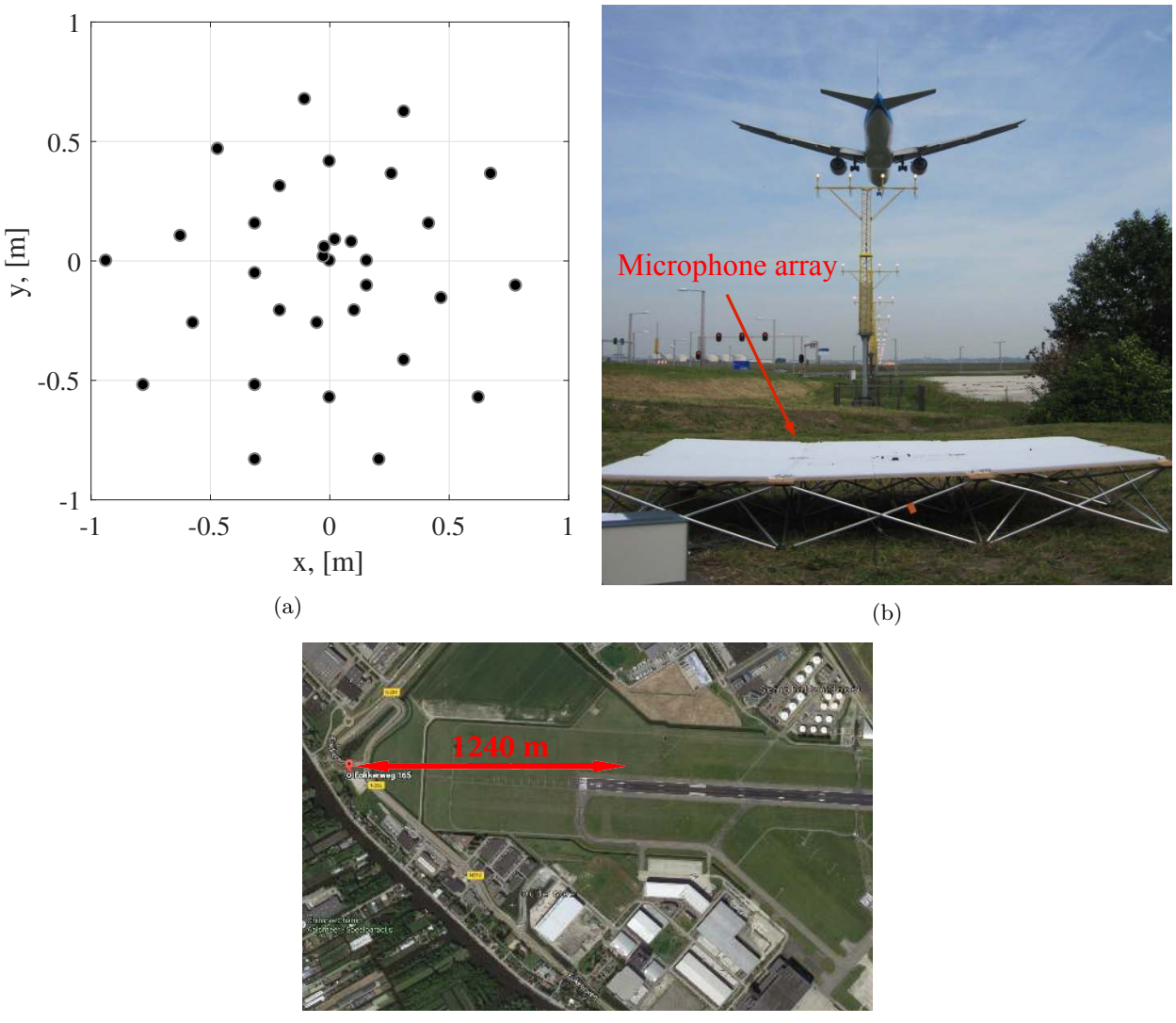

(a) (b) (c)

Figure 1: (a) Microphone distribution for the array used in the flyover measurements [3]. (b) Experimental setup at Amsterdam Airport Schiphol [18]. (c) Location of the microphone array with respect to the Aalsmeerbaan (36R) airport runway. The North is pointing to the right of the picture [21].

and these features are important for flyover measurements, due to the relatively large distance between source and observer [18, 19, 24]. Comparative studies [15, 18] with other acoustic imaging methods showed that functional beamforming provides better results when applied to flyover measurements. This technique raises the source plot obtained with conventional beamforming to the power of an exponent parameter ν and the CSM to the inverse of this power $\frac{1}{\nu}$. The value of ν for this study was selected to be 32 after performing a sensitivity analysis [18, 19].

As mentioned before, only the acoustic data for which the aircraft is overhead of the microphone array ($\theta \approx 90°$) is considered because planar microphone arrays typically show their best performance in their perpendicular direction [40]. This limits the study of the directivity of the different sound sources on board of the aircraft, which is normally of interest due its strong effects in the noise emission levels of some sound sources, such as the turbofan engines. However, landing gear noise is assumed to be almost omnidirectional in the polar direction (θ) [29, 46], so this limitation is less important for this source.

The movement of the aircraft was taken into account in the beamforming formulation [17, 18, 47]. The spherical spreading and the atmospheric absorption of sound were also taken into account to obtain the L_p at the source location [4, 24]. The atmospheric absorption coefficient α was calculated considering the measured ambient temperature, relative humidity and sound frequency, as stated in [48]. The wind speeds and background noise levels were relatively low [22], so it was decided to use the full CSM for the calculations, i.e., without removing its main diagonal, since functional beamforming is quite sensitive to this approach [49].

The obtained source maps were integrated over different regions of integration (ROI) [50, 51] to exclude the influence of other sources outside of these areas. This technique is analogous to the source power integration (SPI) [17, 22, 50–59] but considering the formulation of functional beamforming [21, 22]. This integration process provides the sound emissions for each source. For the calculation of the SQM, the sound signals of each ROI were propagated back to the center of the array, which was considered as the observer location, by accounting for the spherical spreading and atmospheric absorption of sound again.

V. Noise prediction models

This section briefly describes two airframe noise prediction models commonly used to predict landing gear noise. The focus is kept on semi–empirical and semi–analytical noise models typically used for fast estimation of aircraft noise during aircraft design and parametric sensitivity studies, to quantify changes in noise impact due to changes to the aircraft geometry. These models are typically developed based on wind–tunnel or flight measurements of several aircraft and are averaged or normalized to reflect the typical noise spectra and directivities of generic aircraft geometries. As such, their accuracy is limited within a small range of the measurement database on which they are based on. Nonetheless, the models described here have been used extensively by organizations worldwide to assess the community noise impact of various aircraft designs, as well as flight procedures and routes. The computational efficiency of the models to compute the noise impact, in the range of seconds for selected observer points and minutes for ground grids needed to make noise contours, has led to their continuing, widespread use in the noise modeling and prediction communities. Two of the most frequently used models for predicting landing gear noise, that of Fink [31] and Guo [32, 33] are briefly explained here. The detailed formulas for both of these methods and comparisons with experimental data can be found in [22, 60].

V.A. Fink's method

Fink's method [31] was developed for the US Federal Aviation Agency (FAA) and has been implemented in NASA's Aircraft Noise Prediction Program (ANOPP) framework [61, 62]. Fink assumes that there are two primary noise sources on the landing gear: the strut of the gear and the wheels, based on experimental data from flyover measurements of several aircraft [63]. Therefore, the input parameters required for this method are just the mean flow velocity, the number of wheels, the wheel diameter and the strut length which can be normally found in the literature [3, 64]. The various interaction effects of the wheels and the strut with each other as well as with other airframe components are, thus, neglected. The convective amplification due to the movement of the source is taken into account. Different polar and azimuthal sideline (ϕ) emission angles can be calculated, but for this study the direction directly under the landing gear ($\theta = 90°$ and $\phi = 0°$) was used. For these emission angles, the contribution of the strut to the overall noise emissions is expected to be

negligible according to Fink's model [22].

V.B. Guo's method

Also known as the "Boeing" method, Guo's method [32, 33] is based on fundamental aerodynamic noise theory and scaling laws adjusted to fit full–scale LG aeroacoustic tests [60]. In order to include more physics than Fink's method, this technique considers three different types of landing gear components depending on their size, each of them contributing in a different frequency range:

1. Large–scale structures, such as the wheels, contributing to the low–frequency noise.
2. Mid–scale structures, such as the main struts, contributing to the mid–frequency noise.
3. Small–scale structures, such as the hydraulic lines and LG dressings, contributing to the high–frequency noise.

These three components are considered separately with a different spectral shape and directivity. For this purpose, more detailed geometrical inputs are required for this method, compared to Fink's method. Hence, Guo's method is expected to provide higher–fidelity noise predictions. Moreover, the installation effects of the landing gear, such as the presence of the wing and fuselage causing reflections and diffraction, are also considered [33]. As for Fink's method, different polar and azimuthal emission angles can be estimated, but the same aforementioned conditions ($\theta = 90°$ and $\phi = 0°$) were employed in this study.

VI. Experimental results

VI.A. Flyover source plots

As aforementioned, the NLG system of the Airbus A320 is expected to be a dominant noise source during approach and to cause a strong tonal noise [1]. This can be observed in the narrowband frequency spectrum shown in Fig. 2a, which corresponds to the example Airbus A320 flyover considered in this paper. This spectrum indicates the noise emissions of the whole aircraft at the source position (i.e., after propagating the sound back to the emission location, see section IV) and it presents a strong tonal peak at approximately 1720 Hz, protruding more than 10 dB with respect to the surrounding broadband noise. Applying functional beamforming to the microphone array data at that single frequency provides the source plot depicted in Fig. 2b, which confirms that the strong tonal noise is indeed generated at the NLG.

The relative importance of the NLG contribution to the total noise signature of the whole aircraft is confirmed in Fig. 2c where a source plot for the same Airbus A320 flyover is presented. In this case, the results correspond to the whole frequency range of interest (1 kHz to 10 kHz) after applying A–weighting. It can be observed that the NLG is also a dominant noise source for the whole frequency range, as well as the turbofan engines. Other aircraft elements, such as the main landing gear or the high–lift devices also contribute to the overall noise emissions, but their contributions can be excluded to some extent by the integration method explained in section IV. The dashed and dotted black rectangles in Fig. 2c denote the ROIs for the engines and the NLG, respectively.

VI.B. Noise source breakdown

The integrated frequency spectra within the ROIs defined in Fig. 2c, i.e., the NLG and the turbofan engines, are presented in Fig. 3a in one–third–octave bands. The signals extracted from the source maps have been propagated back to the observer position, i.e., the center of the array, as explained in section IV. In addition, the frequency spectrum recorded by the array's center microphone, which basically indicates the total aircraft noise signal (without beamforming applied), is plotted in the same figure. The functional beamforming results considering the whole aircraft were basically the same as those measured by the center microphone for the frequency range of interest. The strong tonal noise shown in Fig. 2a is clearly present in the spectrum of the NLG for the one–third–octave band centered at 1600 Hz and, in a minor way, in the total aircraft noise spectrum. In fact, for that frequency band, the NLG system is the main contributor for aircraft noise as it was observed in Fig. 2b. The spectrum corresponding to the turbofan engines does not present tones as strong as the one of the NLG, but it does show the contribution of the blade passing frequency (BPF) of the fan and its higher harmonics (up to the seventh harmonic). The BPF of this flyover was found to be 1300

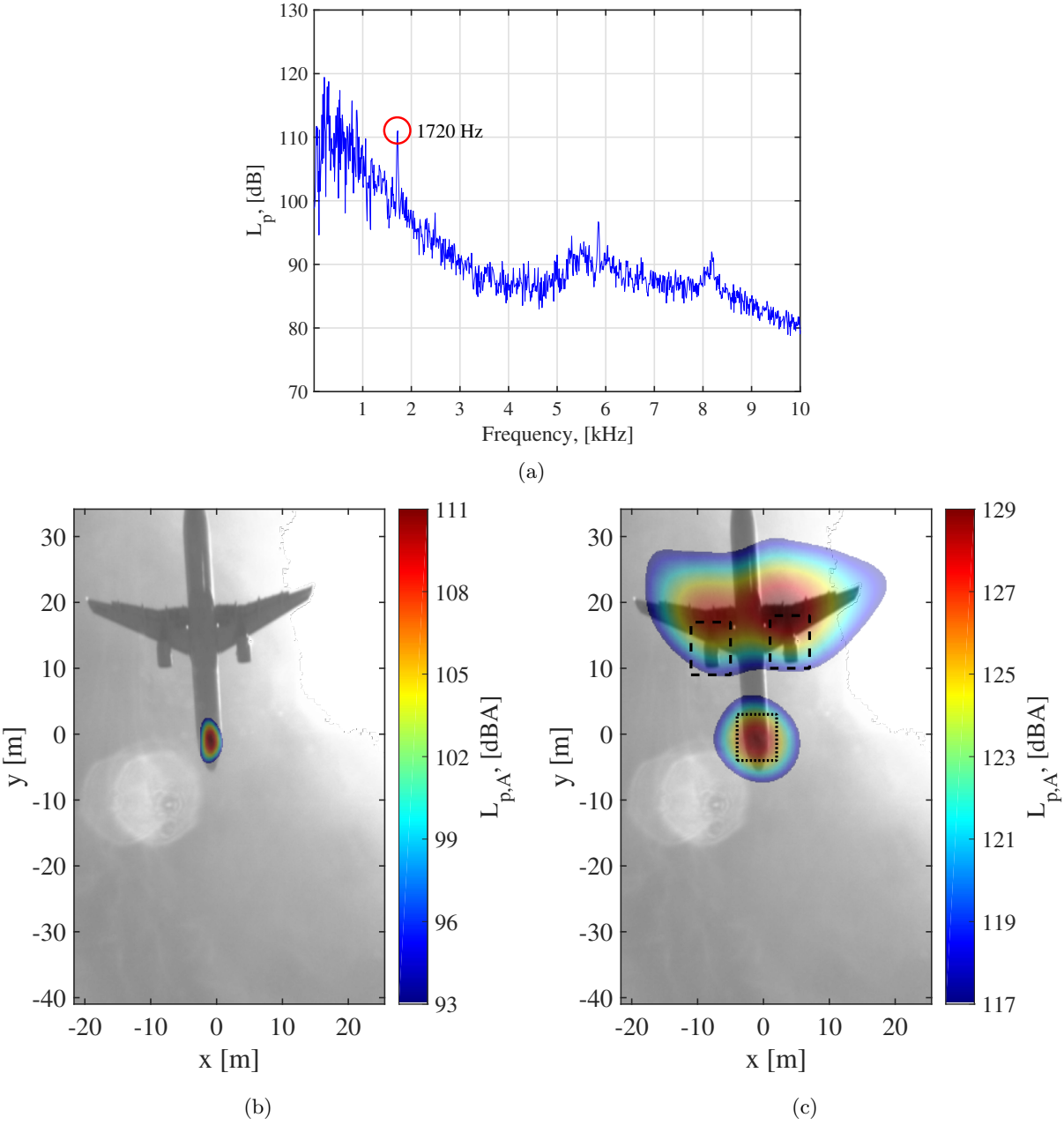

Figure 2: (a) Narrowband frequency spectrum of the Airbus A320 flyover at the source position. Functional beamforming (with $\nu = 32$) source plots (A–weighted) for the same flyover at (b) 1720 Hz and (c) the whole frequency range (1 kHz to 10 kHz). The dashed and dotted black rectangles denote the respective ROIs. Adapted from [3].

Hz at the moment where the aircraft is overhead, corresponding to an engine fan setting of $N1 \approx 43\%$ (with respect to the fan maximum rotational speed) [6, 20, 23, 24]. These tonal components of the fan noise are typically more distinguishable in the forward direction with respect to the aircraft movement, i.e. for polar emission angles $\theta < 90°$ than when the aircraft is directly overhead of the observer [4, 24].

The rest of subfigures in Fig. 3 correspond to bar plots for each SQM considered, as well as for the $L_{\mathrm{p,A}}$ of each of the aircraft elements studied (NLG and turbofan engines) and the total aircraft noise. The first bar plot (Fig. 3b) refers to the $L_{\mathrm{p,A}}$ metric integrated over the frequency range of interest (1 kHz to 10 kHz). The engines show slightly higher values (96.4 dBA) than the NLG (95.4 dBA). The total aircraft noise for this frequency range (100.2 dBA) is almost the same as the combination of the contributions of the NLG and turbofan engines (98.9 dBA), confirming that these two elements are the dominant noise sources on board during landing.

The results for loudness (N) are depicted in Fig. 3c, showing a similar behavior as for the case of $L_{\mathrm{p,A}}$. The engines are louder (104.6 phon) than the NLG (103 phon) and the combination of both sound sources (106.9 phon) is again almost the same as the total aircraft noise (107.8 phon).

The tonality (K) is investigated in Fig. 3d. The most tonal component is clearly the NLG (0.45 t.u.) due to the aforementioned strong tone at 1720 Hz (see Fig. 2a) which is assumed to be caused by an open cavity. The BPF and its harmonics cause the engines to have some tonality as well, but with a lower value (0.15 t.u.). The total aircraft noise presents an intermediate value of 0.27 t.u. most likely due to the masking of the tonal sound of the NLG and the turbofan engines by the broadband noise caused by other elements, which causes the tones to be less prominent compared to the signals of the isolated elements.

Sharpness (S) was considerably similar for the three cases (Fig. 3e) with the engines showing slightly higher values (2.28 acum) compared to the total aircraft (2.21 acum) and the NLG (2.22 acum). The reason for this might be the presence of the higher BPF harmonics for the engine case. Overall, the trends in the spectra for the higher frequency bands ($f > 8$ kHz) is comparable for the three elements, see Fig. 3a.

Lastly, the results for the combined $\mathrm{PA_{mod}}$ metric are gathered in Fig. 3f. Interestingly, it can be observed that, despite having lower values of $L_{\mathrm{p,A}}$ and N, the NLG produces more annoyance (186.3) than the turbofan engines (175.9) because of its considerably higher tonality. This fact highlights the importance of the presence of tonal noise for the expected psychoacoustic annoyance. Dedicated listening tests, however, should be performed in order to confirm this finding.

VI.C. Comparison with airframe noise prediction models

This section compares the characteristics of the sound signal of the NLG obtained experimentally with functional beamforming with the estimations of the prediction models of Fink [31] and Guo [32, 33]. The one–third–octave–band spectra for the three cases are shown in Fig. 4a, where the aforementioned tone is not considered at all by none of the prediction models. A good agreement is found between Fink's model and the experimental data for the 1 kHz band as well as the bands between 2 kHz and 5 kHz. The estimations by Guo's method seem to underestimate the NLG emissions for the whole frequency range. There is also a hump between 5 kHz and 10 kHz in the experimental data that is not well captured by none of the methods. Considerable differences were found in previous research [22] when comparing the experimental results of three other different aircraft types with the estimations of these prediction methods.

The bar plot for the $L_{\mathrm{p,A}}$ metric (Fig. 4b) shows that both Fink's (90.9 dBA) and Guo's (87.4 dBA) estimations are below the experimental value observed (95.4 dBA). These differences are also observed for the loudness metric (Fig. 4c) where the beamforming results show a value of 103 phon and Fink and Guo provide values of 100.5 and 97.4 phon, respectively.

Perhaps the largest difference between the experimental results and the estimations of both methods is regarding the tonality metric (Fig. 4d). Since these models do not consider parasitic noise sources, such as open cavities, they do not provide any tonal noise components and the output spectra are purely broadband. Therefore both modeled spectra have 0 t.u. tonalities compared to the relatively large experimental value (0.45 t.u.).

Once again, the sharpness metric (Fig. 4e) shows similar values between the three approaches (2.21 acum for Fink and 2.17 acum for Guo), since the relative importance of the high–frequency sound with respect to the total loudness of each case was found to be almost the same.

Finally, the obtained values for the $\mathrm{PA_{mod}}$ metric by the noise prediction models are considerably lower (107.3 for Fink and 80.3 for Guo) than the one for the experimental case (186.3). This can be explained by the lower loudness values of the methods' solutions, as well as the lack of any tonality for the predicted spectra

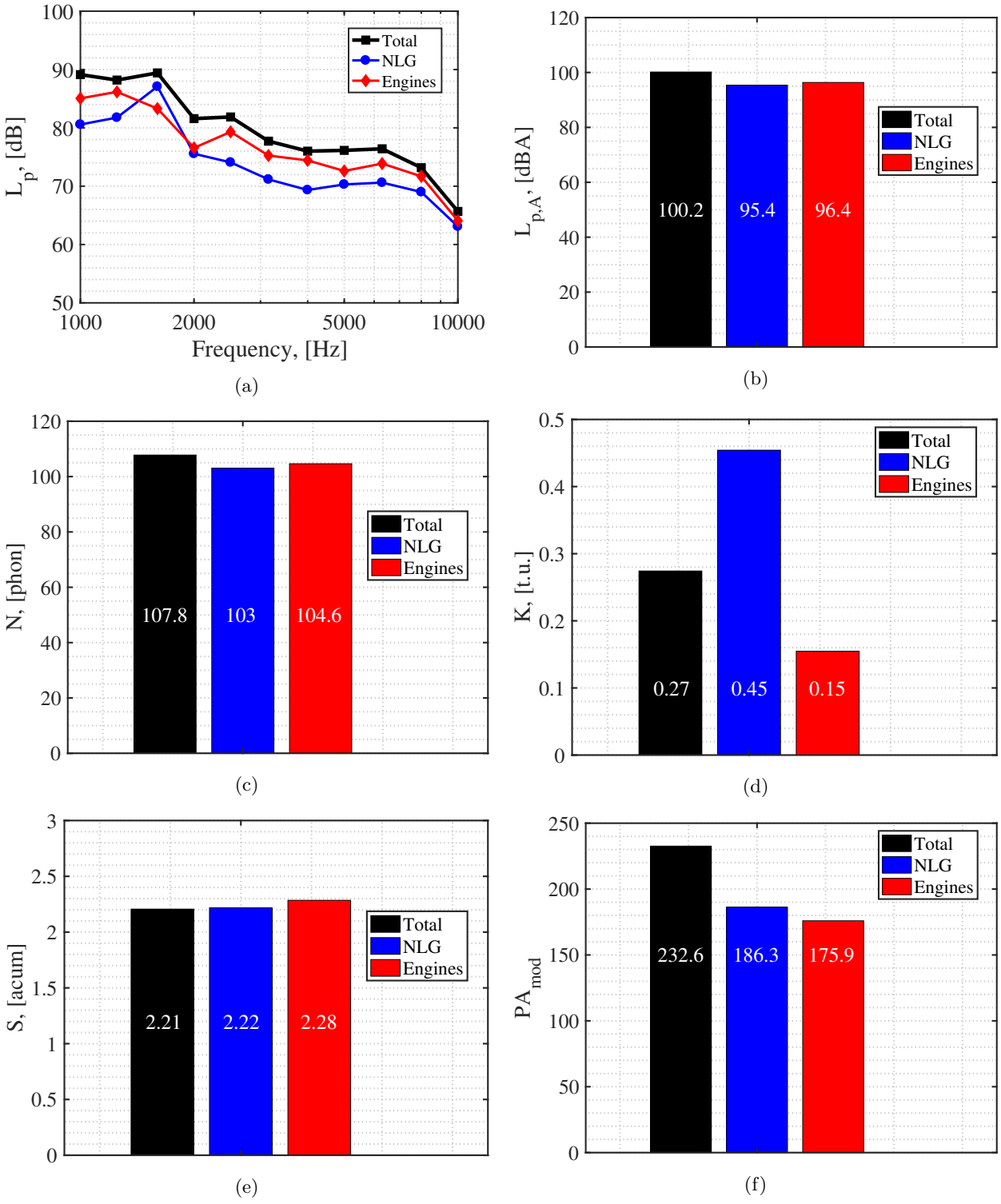

Figure 3: (a) One–third–octave band frequency spectra of the NLG, the turbofan engines and the total aircraft. Bar plots for three cases for: (b) $L_{p,A}$, (c) loudness N, (d) tonality K, (e) sharpness S and (f) modified psychoacoustic annoyance PA_{mod}.

which, as shown in section VI.B, can make a considerable difference in the overall psychoacoustic annoyance. In fact, removing the narrowband tone in the spectrum of the experimental case would considerably reduce the PA_{mod} metric to 137.1, closer to the predictions of the models.

VII. Conclusions

The sound quality of an Airbus A320 aircraft flyover is evaluated in this paper. Since the measurements were performed with a microphone array, it is possible to study the sound emissions of different elements of the aircraft, in this case the nose landing gear (NLG) and the turbofan engines, by applying acoustic imaging methods to the recorded data.

The sound quality metrics (SQM) considered in this work (loudness, tonality and sharpness) can be combined into a overall psychoacoustic annoyance metric (PA_{mod}) that is expected to represent the annoyance experienced by the human ear in a better way than conventional metrics such as the A–weighted sound pressure level ($L_{p,A}$).

It was found that, despite having lower loudness levels, the NLG system caused higher psychoacoustic annoyance than the turbofan engines due to the presence of a very strong tonal sound (and therefore a higher tonality value), which is assumed to be caused by the presence of an open cavity in the NLG system. When comparing the experimental results of the NLG noise emissions with the predictions of the airframe noise models of Fink and Guo, it was found that the models greatly underpredict the noise levels of the NLG and they do not consider the presence of any tonal noise, which leads to a large difference in the predicted actual psychoacoustic annoyance.

Therefore, it is highly recommended to consider more elaborated metrics, such as the SQM used here, to assess aircraft noise emissions in measurements, but also in the design process of novel low–noise aircraft configurations, to ensure that apart from just obtaining a reduction in the sound pressure level in decibels, the perceived annoyance by the population around airports is also decreased. Moreover, noise prediction models should be upgraded to consider tonal noise due to its importance in the psychoacoustic annoyance.

VII.A. Limitations of this research and recommendations

The results presented in this work should be considered as preliminary, since the following limitations need to be noted:

- Only frequencies between 1 kHz and 10 kHz were considered due to limitations of the experimental setup. Lower frequencies can be resolved if a larger microphone array is used, and higher frequencies can be reached if more densely populated arrays are considered. The current frequency range, however, was deemed as appropriate for studying aircraft noise.

- The noise emission directions are limited to when the aircraft is approximately overhead of the observer ($\theta \approx 90°$). Since aircraft are known to be a highly directional sound source [65], the extension of this research to a wider angle range is of high interest. This could be achieved by employing a considerably larger microphone array setup or with a microphone arrangement elongated along the direction of the aircraft movement [66]. In addition, such setup would allow for (at least a short) study of the time evolution of each sound signal, which would allow for the calculation of the time–dependent SQM of roughness and fluctuation strength.

- Just a single Airbus A320 flyover is studied in this paper. This paper is, however, part of ongoing work and the extension to other aircraft types is expected in the near future. Moreover, the study of additional aircraft components (rather than just the NLG and turbofan engines) would be very interesting, since even if they emit lower sound levels they can still have a relatively large contribution to the annoyance experienced. As for the two points above, using a larger array would allow for separating more noise sources, such as the main landing gear.

- In general, all the findings of this research should be confirmed by dedicated listening tests featuring the extracted sound signals of each aircraft element to ensure whether the predicted annoyance corresponds to the actual experienced annoyance by the subjects of the survey.

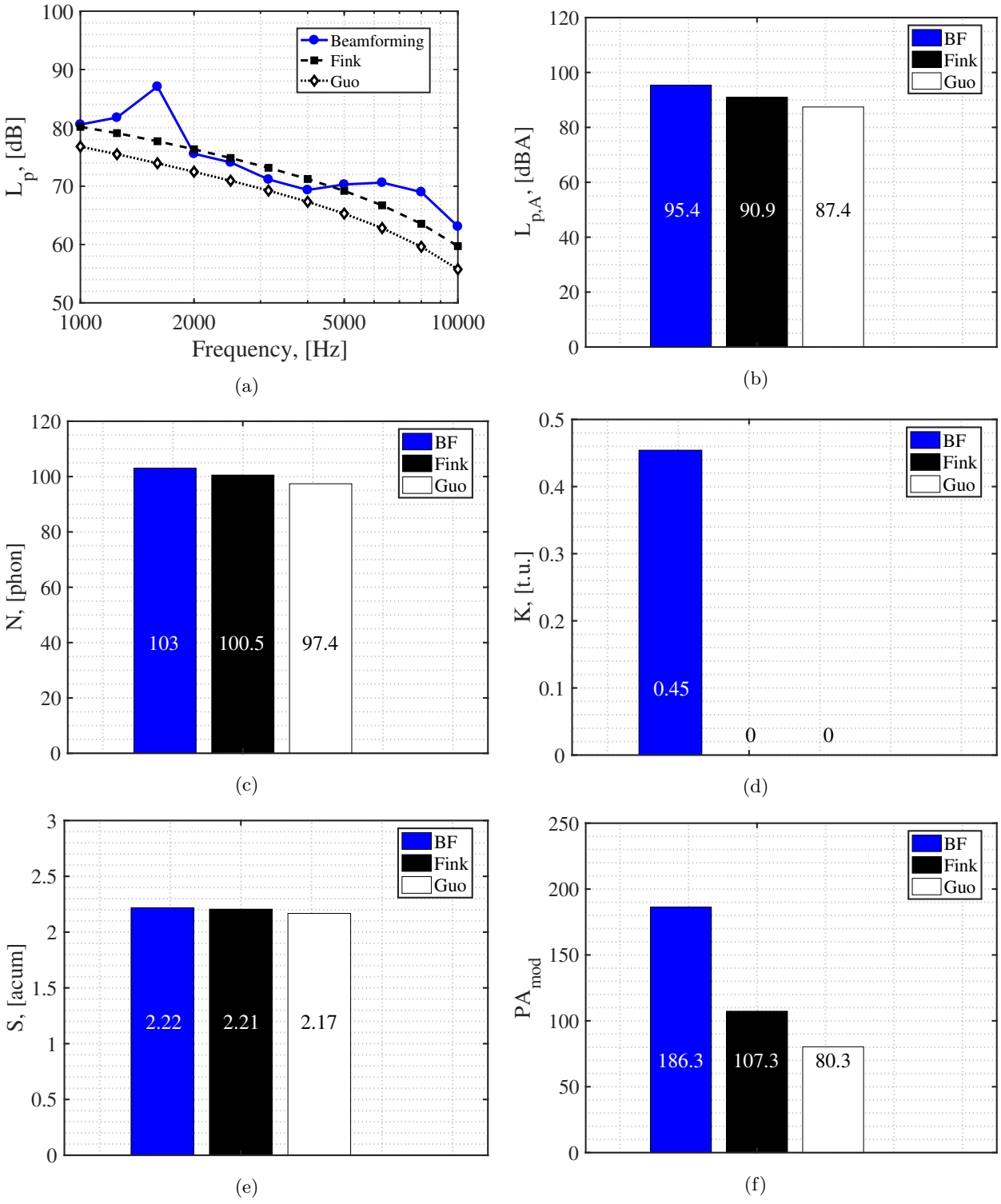

Figure 4: (a) One–third–octave band frequency spectra of the NLG obtained experimentally with beamforming (BF) and with the prediction models of Fink and Guo. Bar plots for three cases for: (b) $L_{p,A}$, (c) loudness N, (d) tonality K, (e) sharpness S and (f) modified psychoacoustic annoyance PA_{mod}.

References

[1] Merino-Martinez, R., Bertsch, L., Snellen, M., and Simons, D. G., "Analysis of landing gear noise during approach," 22^{nd} *AIAA/CEAS Aeroacoustics Conference. May 30 – June 1 2016. Lyon, France*, 2016, AIAA paper 2016–2769.

[2] Hansell, A., Blangiardo, M., Fortunato, L., Floud, S., de, H. K., Fecht, D., Ghosh, R., Laszlo, H., Pearson, C., Beale, L., Beevers, S., Gulliver, J., Best, N., Richardson, S., and Elliott, P., "Aircraft noise and cardiovascular disease near Heathrow airport in London: small area study," *British Medical Journal*, Vol. 347, 2013.

[3] Merino-Martinez, R., *Microphone arrays for imaging of aerospace noise sources*, Ph.D. thesis, Delft University of Technology, 2018, ISBN: 978–94–028–1301–2.

[4] Ruijgrok, G., *Elements of aviation acoustics*, VSSD, Second ed., 2007, ISBN: 1090–6562–155–5.

[5] "Global Market Forecast – Flying by Numbers 2015–2034," Tech. Rep. D14029465, Airbus S.A.S., Blagnac, France, 2015.

[6] Merino-Martinez, R., Heblij, S. J., Bergmans, D. H. T., Snellen, M., and Simons, D. G., "Improving Aircraft Noise Predictions by Considering the Fan Rotational Speed," *Journal of Aircraft*, Vol. 56, No. 1, 2019, pp. 284–294.

[7] Albert, M., Bousquet, P., and Lizarazu, D., "Ground Effects for Aircraft Noise Cerfitication," 23^{rd} *AIAA/CEAS Aeroacoustics Conference. June 5 – 9 2017. Denver, Colorado, USA*, 2017, AIAA paper 2017–3845.

[8] Sahai, A. K. and Stumpf, E., "Incorporating and Minimizing Aircraft Noise Annoyance during Conceptual Aircraft Design," 20^{th} *AIAA/CEAS Aeroacoustics Conference, June 16 – 20 2014, Atlanta, GA, USA*, 2014, AIAA paper 2014–2078.

[9] Sahai, A. K., *Consideration of Aircraft Noise Annoyance during Conceptual Aircraft Design*, Ph.D. thesis, Rheinisch–Westfälische Technische Hochschule Aachen, 2016.

[10] More, S. R., *Aircraft Noise Characteristics and Metrics*, Ph.D. thesis, Purdue University, 2010, Report No. PARTNER–COE–2011–004.

[11] Pereda Albarrán, M. Y., Sahai, A. K., and Stumpf, E., "Aircraft noise sound quality evaluation of continuous descent approaches," 46^{th} *International Congress and Exposition of Noise Control Engineering, 27–30 August, 2017, Hong Kong*, 2017.

[12] Pereda Albarrán, M. Y., Schültke, F., and Stumpf, E., "Sound Quality Assessments of Over–the–Wing Engine Configurations Applied to Continuous Descent Approaches," 24^{th} *AIAA/CEAS Aeroacoustics Conference. June 25 – 29 2018. Atlanta, Georgia, USA*, 2018, AIAA paper 2018–4083.

[13] McGuire, S. and Davies, P., "An overview of methods to quantify annoyance due to noise with application to tire–road noise," Tech. Rep. HL 2008–2 430180000 8000008325–1, American Concrete Pavement Association, February 2008.

[14] Mueller, T., *Aeroacoustic Measurements*, Springer Science & Business Media, 2002, ISBN: 978–3–642–07514–8.

[15] Merino-Martinez, R., Sijtsma, P., Snellen, M., Ahlefeldt, T., Antoni, J., Bahr, C. J., Blacodon, D., Ernst, D., Finez, A., Funke, S., Geyer, T. F., Haxter, S., Herold, G., Huang, X., Humphreys, W. M., Leclère, Q., Malgoezar, A., Michel, U., Padois, T., Pereira, A., Picard, C., Sarradj, E., Siller, H., Simons, D. G., and Spehr, C., "A review of acoustic imaging methods using phased microphone arrays (part of the Aircraft Noise Generation and Assessment special issue)," *CEAS Aeronautical Journal*, Vol. 10, No. 1, March 2019, pp. 197–230, DOI: 10.1007/s13272-019-00383-4.

[16] Michel, U., Barsikow, B., Helbig, J., Hellmig, M., and Schüttpelz, M., "Flyover noise measurements on landing aircraft with a microphone array," 4^{th} *AIAA/CEAS Aeroacoustics Conference, June 2 – 4 1998, Toulouse, France*, 1998, AIAA paper 1998–2336.

[17] Sijtsma, P., "Phased array beamforming applied to wind tunnel and fly–over tests," Tech. Rep. NLR–TP–2010–549, National Aerospace Laboratory (NLR), Anthony Fokkerweg 2, 1059 CM Amsterdam, P.O. Box 90502, 1006 BM Amsterdam, The Netherlands, December 2010.

[18] Merino-Martinez, R., Snellen, M., and Simons, D. G., "Functional beamforming applied to imaging of flyover noise on landing aircraft," *Journal of Aircraft*, Vol. 53, No. 6, November–December 2016, pp. 1830–1843.

[19] Merino-Martinez, R., Snellen, M., and Simons, D. G., "Functional Beamforming Applied to Full Scale Landing Aircraft," 6^{th} *Berlin Beamforming Conference, February 29 – March 1 2016, Berlin, Germany*, GFaI, e.V., Berlin, 2016, BeBeC–2016–D12.

[20] Merino-Martinez, R., Snellen, M., and Simons, D. G., "Determination of Aircraft Noise Variability Using an Acoustic Camera," 23^{rd} *International Congress on Sound and Vibration, July 10 – 14 2016, Athens, Greece*, International Inst. of Acoustics and Vibration (IIAV), Auburn, Alabama, USA., July 2016.

[21] Merino-Martinez, R., Neri, E., Snellen, M., Kennedy, J., Simons, D. G., and Bennett, G. J., "Comparing flyover noise measurements to full–scale nose landing gear wind–tunnel experiments for regional aircraft," 23^{rd} *AIAA/CEAS Aeroacoustics Conference. June 5 – 9 2017. Denver, Colorado, USA*, 2017, AIAA paper 2017–3006.

[22] Merino-Martinez, R., Neri, E., Snellen, M., Kennedy, J., Simons, D. G., and Bennett, G. J., "Analysis of nose landing gear noise comparing numerical computations, prediction models and flyover and wind–tunnel measurements," 24^{th} *AIAA/CEAS Aeroacoustics Conference. June 25 – 29 2018. Atlanta, Georgia, USA*, 2018, AIAA paper 2018–3299.

[23] Snellen, M., Merino-Martinez, R., and Simons, D. G., "Assessment of aircraft noise sources variability using an acoustic camera," 5^{th} *CEAS Air & Space Conference. Challenges in European Aerospace. September 7 – 11 2015, Delft, Netherlands*, No. Paper 2015–019, Council of European Aerospace Societies, September 2015.

[24] Snellen, M., Merino-Martinez, R., and Simons, D. G., "Assessment of noise level variability on landing aircraft using a phased microphone array," *Journal of Aircraft*, Vol. 54, No. 6, 2017, pp. 2173–2183.

[25] Vieira, A., Mehmood, U., Merino-Martinez, R., Snellen, M., and Simons, D. G., "Variability of sound quality metrics for different aircraft types during landing and take–off," 25^{th} *AIAA/CEAS Aeroacoustics Conference. May 20 – 24 2019. Delft, The Netherlands*, 2019, AIAA paper 2019–2512.

[26] Bertsch, L., *Noise Prediction within Conceptual Aircraft Design*, Ph.D. thesis, DLR, 2013, DLR Forschungsbericht, ISRN DLR–FB–2013–20, ISSN 1434–8454.

[27] Dedoussi, I., Hynes, T., and Siller, H., "Investigating landing gear noise using fly–over data: the case of a Boeing 747–400," 19^{th} *AIAA/CEAS Aeroacoustics Conference, May 27 – 29, 2013, Berlin, Germany*, 2013, AIAA paper 2013–2115.

[28] De Metz, F. C. and Farabee, T. M., "Laminar and Turbulent Shear Flow Induced Cavity Resonances," 4^{th} *AIAA Aeroacoustics Conference. October 3 – 5 1977, Atlanta, Georgia, USA*, 1977, AIAA paper 1977–1293.

[29] Michel, U. and Qiao, W., "Directivity of Landing–Gear Noise Based on Flyover Measurements," 5^{th} *AIAA/CEAS Aeroacoustics Conference, May 10 – 12 1999, Bellevue, Greater Seattle, WA, USA*, 1999, AIAA paper 1999–1956.

[30] Dobrzynski, W., "Almost 40 Years of Airframe Noise Research: What Did We Achieve?" *Journal of Aircraft*, Vol. 47, No. 2, March–April 2010, pp. 353–367.

[31] Fink, M. R., "Noise component method for airframe noise," 4^{th} *AIAA Aeroacoustics Conference. October 3 – 5 1977, Atlanta, Georgia, USA*, 1977, AIAA paper 1977–1271.

[32] Guo, Y., "Empirical Prediction of Aircraft Landing Gear Noise," Tech. Rep. NASA TM–2005–213780, NASA, July 2005.

[33] Guo, Y., "A Semi–Empirical Model for Aircraft Landing Gear Noise Prediction," 12^{th} *AIAA/CEAS Aeroacoustics Conference. May 8 – 10 2006, Cambridge, Massachusetts, USA*, 2006, AIAA paper 2006–2627.

[34] Brandt, A., *Noise and vibration analysis: signal analysis and experimental procedures*, Second, John Wiley & Sons, 2011, ISBN: 978-0-470-74644-8.

[35] "ISO norm 532–1 – Acoustics – Method for calculating loudness – Zwicker method," Tech. Rep. 1, International Organization for Standardization, 2017.

[36] Aures, W., "Procedure for calculating the sensory euphony of arbitrary sound signal," *Acustica*, Vol. 59, No. 2, 1985, pp. 130–141.

[37] von Bismark, G., "Sharpness as an attribute of the timbre of steady sounds," *Acta Acustica united with Acustica*, Vol. 30, No. 3, 1974, pp. 159–172.

[38] Fastl, H. and Zwicker, E., *Psychoacoustics – Facts and models*, Springer Series in Information Sciences, Third ed., 2007, ISBN: 987–3–540–68888–4.

[39] Daniel, P. and Webber, R., "Psychoacoustical Roughness: Implementation of an Optimized Model," *Accustica – acta acustica*, Vol. 83, 1997, pp. 113–123.

[40] Oerlemans, S., *Detection of aeroacoustic sound sources on aircraft and wind turbines*, Ph.D. thesis, University of Twente, Enschede, the Netherlands, 2009.

[41] PUI Audio POM–2735P–R microphone website, "http://www.puiaudio.com/product-detail.aspx?categoryId=4&partnumber=POM-2735P-R," Accessed in January 2017.

[42] Datavision UI-1220LE optical camera website, "https://en.ids-imaging.com/store/ui-1220le.html," Accessed in January 2015.

[43] Welch, P. D., "The Use of Fast Fourier Transform for the Estimation of Power Spectra: A Method Based on Time Averaging Over Short, Modified Periodograms," *IEEE Transactions on Audio and Electroacoustics*, Vol. AU–15, No. 2, June 1967, pp. 70–73.

[44] Dougherty, R. P., "Functional Beamforming," 5^{th} *Berlin Beamforming Conference, February 19 – 20 2014, Berlin, Germany*, GFaI, e.V., Berlin, 2014.

[45] Dougherty, R. P., "Functional Beamforming for Aeroacoustic Source Distributions," 20^{th} *AIAA/CEAS Aeroacoustics Conference. June 16 – 20 2014. Atlanta GA, USA*, 2014, AIAA paper 2014–3066.

[46] Dobrzynski, W. and Buchholz, H., "Full–scale noise testing on Airbus landing gears in the German Dutch Wind Tunnel," 3^{rd} *AIAA/CEAS Aeroacoustics Conference. May 12 – 14 1997, Atlanta GA, USA*, 1997, AIAA paper 1997–1597.

[47] Howell, G. P., Bradley, M. A., McCormick, M. A., and Brown, J. D., "De–Dopplerization and acoustic imaging of aircraft flyover noise measurements," *Journal of Sound and Vibration*, Vol. 105, No. 1, Feb 1986, pp. 151–167.

[48] Rossing, T. D., *Handbook of Acoustics*, Springer Science & Business Media, Second ed., 2007, ISBN: 987–0–387–30446–5.

[49] Dougherty, R. P., "Cross Spectral Matrix Diagonal Optimization," 6^{th} *Berlin Beamforming Conference, February 29 – March 1, 2016, Berlin, Germany*, GFaI, e.V., Berlin, 2016.

[50] Merino-Martinez, R., Sijtsma, P., and Snellen, M., "Inverse Integration Method for Distributed Sound Sources," 7^{th} *Berlin Beamforming Conference, March 5 – 6 2018, Berlin, Germany*, GFaI, e.V., Berlin, 2018, BeBeC–2018–S07.

[51] Merino-Martinez, R., Sijtsma, P., Rubio Carpio, A., Zamponi, R., Luesutthiviboon, S., Malgoezar, A. M. N., Snellen, M., Schram, C., and Simons, D. G., "Integration methods for distributed sound sources," *International Journal of Aeroacoustics*, 2019, DOI: 10.1177/1475472X19852945.

[52] Merino-Martinez, R., Sanders, M. P. J., Caldas, L. C., Avallone, F., Ragni, D., de Santana, L. D., Snellen, M., and Simons, D. G., "Comparison between analog and digital microphone phased arrays for aeroacoustic measurements," 24^{th} *AIAA/CEAS Aeroacoustics Conference. June 25 – 29 2018. Atlanta, Georgia, USA*, 2018, AIAA paper 2018–2809.

[53] Arce León, C., Merino-Martinez, R., Ragni, D., Avallone, F., and Snellen, M., "Boundary layer characterization and acoustic measurements of flow–aligned trailing edge serrations," *Experiments in Fluids*, Vol. 57, No. 182, October 2016, pp. 1 – 22.

[54] Arce León, C., Merino-Martinez, R., Ragni, D., Avallone, F., Scarano, F., Pröbsting, S., Snellen, M., Simons, D. G., and Madsen, J., "Effect of trailing edge serration–flow misalignment on airfoil noise emission," *Journal of Sound and Vibration*, Vol. 405, May 2017, pp. 19 – 33.

[55] Arce León, C., Merino-Martinez, R., Pröbsting, S., Ragni, D., and Avallone, F., "Acoustic Emissions of Semi–Permeable Trailing Edge Serrations," *Acoustics Australia*, Vol. 46, No. 1, 2017, pp. 111–117.

[56] Arce León, C., Merino-Martinez, R., Ragni, D., Pröbsting, S., Avallone, F., Singh, A., and Madsen, J., "Trailing Edge Serrations – Effect of Their Flap Angle on Flow and Acoustics," 7^{th} *International Meeting on Wind Turbine Noise, May 2 – 5 2017, Rotterdam, the Netherlands*, 2017.

[57] Rubio Carpio, A., Merino-Martinez, R., Avallone, F., Ragni, D., Snellen, M., and van der Zwaag, S., "Broadband Trailing Edge Noise Reduction Using Permeable Metal Foams," 46^{th} *International Congress and Exposition of Noise Control Engineering, 27–30 August, 2017, Hong Kong*, 2017.

[58] Rubio Carpio, A., Merino-Martinez, R., Avallone, F., Ragni, D., Snellen, M., and van der Zwaag, S., "Experimental characterization of the turbulent boundary layer over a porous trailing edge for noise abatement," *Journal of Sound and Vibration*, Vol. 443, March 2019, pp. 537–558.

[59] Sarradj, E., Herold, G., Sijtsma, P., Merino-Martinez, R., Malgoezar, A. M. N., Snellen, M., Geyer, T. F., Bahr, C. J., Porteous, R., Moreau, D. J., and Doolan, C. J., "A microphone array method benchmarking exercise using synthesized input data," 23^{rd} *AIAA/CEAS Aeroacoustics Conference. June 5 – 9 2017. Denver, CO, USA*, 2017, AIAA paper 2017–3719.

[60] Burley, C. L., Brooks, T. F., Humphreys Jr., W. M., and W., R. J. J., "ANOPP Landing Gear Noise Prediction Comparisons to Model–Scale Data," 13^{th} *AIAA/CEAS Aeroacoustics Conference (*28^{th} *AIAA Aeroacoustics Conference), May 21 – 23 2017, Rome, Italy*, 2007, AIAA paper 2007–3459.

[61] Zorumski, W. E., "Aircraft Noise Prediction Program – Theoretical Manual – Part 1," Tech. Rep. NASA Technical Memorandum 83199, NASA Technical Memorandum 83199, 1982.

[62] Zorumski, W. E., "Aircraft Noise Prediction Program – Theoretical Manual – Part 2," Tech. Rep. NASA Technical Memorandum 83199, NASA Technical Memorandum 83199, 1982.

[63] Heller, H. H. and Dobrzynski, W. M., "Sound Radiation from Aircraft Wheel–Well/Landing–Gear Configuration," *Journal of Aircraft*, Vol. 14, No. 8, 1977, pp. 768–774.

[64] "Airbus A320 Aircraft Characteristics. Airport and Maintenance Planning," Tech. rep., Airbus S.A.S., Blagnac, France., 2005.

[65] Arntzen, M., *Aircraft noise calculation and synthesis in a non–standard atmosphere*, Ph.D. thesis, Delft University of Technology, 2014, ISBN: 978–94–62594–64–7.

[66] Reed, D., Herkes, W., and Shivashankara, B., "The Boeing Quiet Technology Demonstrator Program," 25^{th} *International Congress of the Aeronautical Sciences (ICAS)*, 2006.